

Cavity cooling of a microlever

Constanze Hühberger Metzger & Khaled Karrai

Center for NanoScience and Sektion Physik, Ludwig-Maximilians-Universität, Geschwister-Scholl-Platz 1, 80539 München, Germany

The prospect of realizing entangled quantum states between macroscopic objects and photons¹ has recently stimulated interest in new laser-cooling schemes^{2,3}. For example, laser-cooling of the vibrational modes of a mirror can be achieved by subjecting it to a radiation² or photothermal⁴ pressure, actively controlled through a servo loop adjusted to oppose its brownian thermal motion within a preset frequency window. In contrast, atoms can be laser-cooled passively without such active feedback, because their random motion is intrinsically damped through their interaction with radiation^{5–8}. Here we report direct experimental evidence for passive (or intrinsic) optical cooling of a micro-mechanical resonator. We exploit cavity-induced photothermal pressure to quench the brownian vibrational fluctuations of a gold-coated silicon microlever from room temperature down to an effective temperature of 18 K. Extending this method to optical-cavity-induced radiation pressure might enable the quantum limit to be attained, opening the way for experimental investigations of macroscopic quantum superposition states¹ involving numbers of atoms of the order of 10¹⁴.

The gold-coated silicon micro-cantilever forms one of the two mirrors of a miniature Fabry–Pérot (FP) optical cavity in a set-up shown in Fig. 1. When the FP cavity is tuned near one of its optical resonances, the density of photons stored in it is resonantly enhanced. Equilibrium is reached only after a time when the flux of stored photons equals the photon leakage, which is entirely determined by the mirrors' transmission as well as the mirror separation. As the lever is mechanically flexible, it moves under the effect of the resonantly increased photon-induced forces. So when subjected to a strong enough laser field, the lever mirror displacement affects in turn the photon density stored in the FP cavity. In this way the lever mechanics is strongly coupled to the light field. Such a concept has been explored in pioneering work^{9,10} and later verified with laser fields¹¹. We recently demonstrated that the effect is also seen in lever-based microcavities¹². During the lever motion, the photon leakage rate in the FP cavity changes as well. Because this change is not instantaneous but delayed, it leads to a force experienced by the lever that is proportional to its velocity⁹. Here we demonstrate experimentally that such a light-induced viscous damping is responsible for the cavity cooling of the lever.

First we show how laser-induced cooling is monitored. As the brownian motion of the lever is a measure of its temperature, we have analysed quantitatively the noise spectrum in the cantilever thermal-induced motion in the vicinity of the lowest lever vibrational resonance frequency at 7.3 kHz. As attested by the remarkable behaviour shown in Fig. 2a (obtained for a slightly blue detuned FP cavity using a lever placed in vacuum), we found that increasing laser power reduces the amplitude of the brownian motion by almost two orders of magnitude. In other words, the lever behaves as if it were refrigerated. The advantage of this method is that the lever geometry, the materials used and the FP cavity size are parameters that can be engineered to optimize cavity cooling.

We derive now a model that accounts quantitatively for the observed cooling of the vibrational mode. The displacement z of the cantilever from its equilibrium position obeys Newton's equation of motion. As the cantilever has an elastic rigidity K , its equation of motion for small amplitudes z can be approximated by that of a driven damped harmonic oscillator with an effective mass¹³ m . An effective thermal force F_{th} in the equation of motion¹⁴ drives

the lever into brownian motion. Crucial to the present cooling scheme is the fact that the lever is also subjected to photon-induced forces that depend on the FP cavity length and are hence a function of the lever displacement z . The photon-induced force $F(z) = \sum_n F_n(z)$, which is assumed proportional to the light intensity stored in the cavity, includes of course the radiation pressure but more generally all the n independent light-induced contributions, such as the photothermal (bolometric), radiometric and photo-elastic pressure to name just a few. For instance, a bolometric force F_B results from the differential thermal expansion between the silicon lever and the thin gold film (refs 12, 15 and 16, and ref. 17 and refs therein). When photons are absorbed in the gold film, the composite gold/silicon lever heats locally and bends, thereby changing the cavity length. As we will see below, the essence of cooling is based on the fact that the optically induced forces acting on the lever are delayed with respect to a sudden change in the lever position. To take this delayed response into account, we define $h_n(t - t')$, which is the response function that gives the force contribution F_n at time t for a sudden change $z(t')$ at time t' . The equation of motion is

$$m \frac{d^2 z}{dt^2} + m\Gamma \frac{dz}{dt} + Kz = F_{th} + \sum_n \int_0^t \frac{dF_n[z(t')]}{dt} h_n(t - t') dt' \quad (1)$$

where the damping factor Γ accounts for the mechanical energy loss inherent to the microlever. We have assumed exponential delayed responses, $h_n(t) = 1 - \exp(-t/\tau_n)$, where τ_n is the time it takes for the light-induced force F_n to reach equilibrium after a sudden change in z .

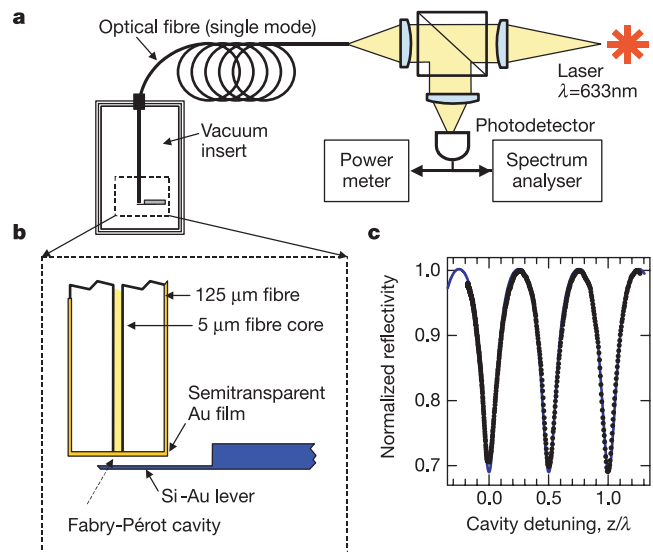


Figure 1 Experimental set-up. **a**, The light of a HeNe laser with wavelength $\lambda = 633$ nm is launched into a single-mode fibre. The other end of the fibre is in a vacuum chamber (10^{-6} mbar)—this end is polished and coated with a gold semitransparent thin film. **b**, The flat end of the fibre makes one of the two mirrors of a Fabry–Pérot cavity. The second mirror is made out of a thin silicon microlever 223 μm long, 22 μm broad and 0.46 μm thick, corresponding to a nominal elastic constant of $K = 0.008 \text{ N m}^{-1}$. Both faces of the cantilever are coated with ~ 35 -nm-thick gold films, so that a slight asymmetry in the film thickness leads to a photo-thermal induced force. The nominal separation between the two mirrors is $\sim 34 \mu\text{m}$. The light reflected from the FP cavity retraces its way back through the fibre, through a beam splitter to a photodetector. In order to avoid spurious effects, the laser was optically isolated from the lever so that less than 1 in 10^5 parts of the reflected signal returned to the source. **c**, The measured reflected light power plotted as a function of the mirror distance shows FP resonances (dots). The line through the data is the best fit to a model for a cavity with both mirrors reflecting 40% each. The cavity detuning length z is adjusted electrostatically by applying a DC voltage between the gold film coating the fibre and the lever¹². A spectrum analyser (0–100 kHz) is used to acquire the thermal noise spectrum in the region close to the lowest vibrational resonance of the lever.

We solve equation (1) in the limit of small lever amplitudes z typical of brownian fluctuations. In this case, the photon-induced force can be approximated by its two first terms in Taylor expansion around the lever's equilibrium position, namely $F(z) \approx \Sigma_n(F_{0n} + [\partial F/\partial z]_{0n}z)$. The first term is the optical driving force, the DC component of which displaces the lever to a new equilibrium position. The second term, which can be positive or negative depending on the cavity detuning^{9,12}, is proportional to the lever displacement. This means that the second term can be identified with elastic forces with photon-induced rigidities^{9,12} $K_n = -[\partial^2 F/\partial z^2]_{0n}$ that add to the lever mechanical elastic rigidity K . $K_n = 0$ for cavities exactly tuned on optical resonance, and K_n extremal values (which are proportional to the light intensity and the third power of the cavity finesse¹²), are obtained by slightly detuning the cavity. The equation of motion decomposed in the frequency domain f has then a simple solution for the lever amplitude components z_ω at cyclic frequency $\omega = 2\pi f$ given by

$$z_\omega = \frac{\sum_n \Delta F_{0n,\omega}/(1+i\omega\tau_n) + F_{th,\omega}}{K} \frac{\omega_0^2}{\omega_{eff}^2 - \omega^2 + i\Gamma_{eff}\omega} \quad (2)$$

where $\Delta F_{0n,\omega}$ and $F_{th,\omega}$ are the Fourier components of a weakly modulated driving force ΔF_{0n} and of F_{th} , respectively. $\omega_0^2 = K/m$ is the lowest vibrational resonance of the lever in the absence of illumination. The above expression is that of the amplitude spectrum of a driven harmonic oscillator with an optically modified damping Γ_{eff} and a modified resonance frequency ω_{eff} given by

$$\Gamma_{eff} = \Gamma \left(1 - Q_M \sum_n \frac{\omega_0 \tau_n}{\omega^2 \tau_n^2 + 1} \frac{K_n}{K} \right) \quad (3)$$

$$\omega_{eff}^2 = \omega_0^2 \left(1 + \sum_n \frac{1}{\omega^2 \tau_n^2 + 1} \frac{K_n}{K} \right) \quad (4)$$

where $Q_M = \omega_0/\Gamma$ is the mechanical quality factor of the lever vibrational resonance, which here is typically of the order of 2×10^3 in vacuum, but as shown in ref. 18, it can be made as large as 2×10^5 .

From equation (3), we see that the photo-induced change in the viscous damping is controlled through the light-induced force rigidity K_n and the delay τ_n . In particular, when operating on cavity

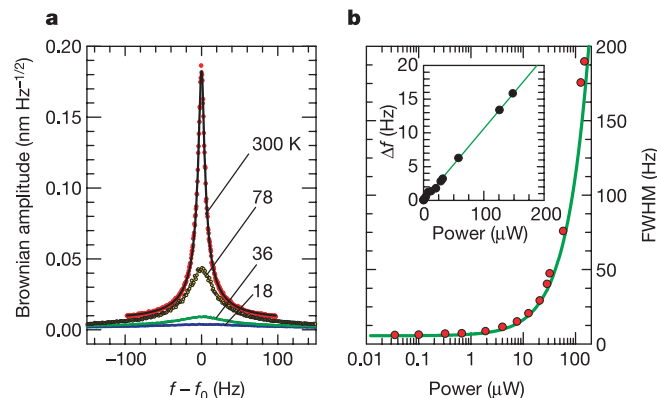


Figure 2 Cavity-induced cooling of the lever vibrational resonance. **a**, Brownian motion amplitude spectra of the lever vibrational resonance measured for four different laser power levels. The largest peak spectrum data (dots) centred on $\omega_0 = 2\pi \times 7,280$ Hz was obtained at 80 nW. The full line is the calculated brownian noise spectrum using a temperature $T = 300$ K. Increasing the laser power to 130 μ W reduced markedly the area of the peak and shifted its frequency to $\omega_{eff} = 2\pi \times 7,300$ kHz. The spectra calculated using equations (5) and (7) fit perfectly the data obtained at three different increasing laser powers when effective temperatures $T_{eff} = 78, 36$ and 18 K are assumed. The cantilever amplitude calibration is obtained independently using the measured interferogram shown in Fig. 1c. The FP cavity was $+\lambda/25$ detuned from one of its optical resonances. **b**, Full-width at half-maximum (FWHM) of the vibrational resonance as a function of the power reflected from the cavity. The full line is a fit according to equation (3). Inset: frequency shift of the resonance. The full line is a fit according to equation (4).

detuning such that $K_n < 0$, equation (3) shows that Γ_{eff} increases linearly with K_n and hence with the photon intensity in the cavity. This behaviour is directly experimentally confirmed in Fig. 2b, where the linewidth of the vibrational resonance is seen to increase with the laser power coupled into the cavity. A further consistency check is obtained by changing the sign of detuning such that $K_n > 0$. In this situation, a value of the product $Q_M \tau_n K_n$ can be reached that nulls the effective damping Γ_{eff} and even makes it negative. When such a situation is reached, the lever is no longer damped and thermal fluctuations are strong enough to set it into a mode of self-oscillation. Such instabilities were first explored in refs 9 and 10 and are often discussed in relation to large optomechanical systems, such as a gravitational wave antenna¹⁹. Under a condition of red detuning, we indeed observed (just as predicted) that above a threshold of laser intensity the lever enters into a mode of self-oscillation at the resonance frequency. The corresponding resonance is seen in Fig. 3c.

The lever was placed in high vacuum so that only the radiation and bolometric pressure are expected to dominate. In order to determine their relative contribution, we measured the full spectrum of z_ω (not shown) over five decades in frequency, from 1 Hz to 100 kHz, by weakly modulating the laser intensity. In our particular device, the distance between both mirrors (34 μ m) is short enough, and the mirrors' reflectivities are low enough, that a change in the lever position leads to an instantaneous change in the photon intensity in the cavity. Therefore, the radiation pressure changes quasi-instantaneously with fluctuations of the lever position, and the cavity-induced damping seen in Fig. 2b is dominated by the bolometric contribution alone. Fitting equation (2) to the measured

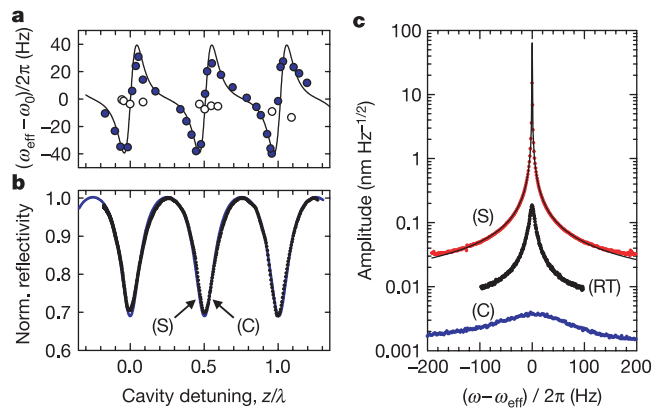


Figure 3 Lever vibrational resonance frequency and shape as a function of the optical cavity tuning. **a**, Frequency shift of the lowest mechanical lever resonance as a function of the FP cavity detuning (here measured at room pressure). The data (filled circles) measured at 100 μ W laser power show a clear periodic dependency with the cavity length, demonstrating optical control of the mechanical resonance. The FP reflectivity resonances shown for direct comparison in **b** have the same periodicity. In contrast, the data (open circles in **a**) measured at lower laser power (5 μ W) show no effect. The vibrational frequencies are obtained by fitting the spectral noise amplitude to equation (5). The fit (full line in **a**) is given using equation (4) together with the photon-induced rigidity $K_{ph} = kF_0(g^3/\sqrt{R})\text{sinc}kz_0\text{cos}kz_0/(1 + g^2\text{sinc}kz_0)^2$ from ref. 12, where $k = 2\pi/\lambda$, F_0 is the light-induced force that the lever would experience in the absence of the FP cavity, z_0 is the equilibrium mirror separation, and $g = 2\sqrt{R}/T$ is the FP cavity finesse assuming that both mirrors have a transmission R and reflectivity T . **c**, Brownian amplitude noise spectrum of the lever near the lowest vibrational resonance frequency, measured under vacuum conditions with 130 μ W laser power. Cooling, demonstrated in curve (C), is obtained by detuning the cavity length by about $+\lambda/25$ from an FP optical resonance (working point shown by an arrow labelled (C) in **b**). Self-excitation, shown by curve (S), in contrast, is obtained by detuning the cavity length by about $-\lambda/25$ (working point (S) indicated by arrow in **b**). The curve labelled (RT) is the room-temperature brownian motion amplitude obtained at 80 nW laser power. The data in **c** are fitted using equation (5) together with equations (3) and (4).

z_ω spectrum, we obtained the response time of the bolometric force, $\tau_B = 560 \mu\text{s}$, and the ratio of the bolometric to radiation pressure contribution, $F_{B0}/F_{R0} = K_B/K_R = -95$, indicating that for this particular gold-coated lever, bolometric forces and radiation pressure act in opposite directions. Investigating the behaviour of the vibrational resonance frequency further strengthens the consistency of our analysis. Equation (4) shows that all light rigidities K_n contribute to modify the lever resonance frequency. However, in the present case for the frequency range centred on the lever vibrational resonance frequency $\omega \approx \omega_0 = 2\pi \times 7.3 \text{ kHz}$, the denominator $(\omega_0\tau_B)^2 + 1 \approx 626$ reduces the bolometric contribution so much that the light-induced shift in the effective resonance frequency ω_{eff} is fully dominated by the radiation pressure. Tuning the cavity length changes periodically the radiation-pressure-induced rigidity K_R from positive to negative values, increasing or decreasing the mechanical resonance frequency, just as observed in Fig. 3a.

Damping does not necessarily imply cooling. To see how the temperature can be lowered, we analyse the effects of cavity-induced damping on the brownian vibrational motion of the lever. When the laser source intensity is kept constant in time ($\Delta F_{0n,\omega} = 0$ for $\omega \neq 0$), the lever is only thermally driven and its mechanical resonance is revealed in the noise spectrum of the light reflected from the microcavity, as shown in Fig. 2. The effective lever temperature is obtained by considering the mean square of the spectral components of the thermal driving force¹⁴ F_{th} in a frequency window $\delta f = \delta\omega/2\pi$. The result gives the frequency component of the mean of the lever's squared amplitude:

$$\langle z_\omega^2 \rangle = \frac{4k_B T}{K} \frac{\omega_0^2 \Gamma}{(\omega_{\text{eff}}^2 - \omega^2)^2 + (\Gamma_{\text{eff}} \omega)^2} \delta f \quad (5)$$

Integrating it over the whole frequency spectrum, we obtain the mean of the lever noise squared amplitude, which relates directly to the lever mean kinetic energy. In our experimental situation, $\omega_{\text{eff}} \approx \omega_0$ and $\Gamma_{\text{eff}} \ll \omega_0$, the result approximates to

$$\frac{1}{2} K \langle z^2 \rangle \cong \frac{1}{2} k_B T \left(\frac{\omega_0^2}{\omega_{\text{eff},0}^2} \frac{\Gamma}{\Gamma_{\text{eff},0}} \right) \quad (6)$$

where $\omega_{\text{eff},0}$ and $\Gamma_{\text{eff},0}$ are the values of ω_{eff} and Γ_{eff} given in equations (3) and (4) setting $\omega = \omega_0$. This expression can be identified with the equipartition theorem for a one-dimensional harmonic oscillator at an effective temperature given by:

$$T_{\text{eff}} = T \frac{\omega_0^2}{\omega_{\text{eff},0}^2} \frac{\Gamma}{\Gamma_{\text{eff},0}} \quad (7)$$

This expression demonstrates that a control of the mechanical oscillator's temperature is obtained through cavity tuning of both the effective vibrational resonance frequency and the effective damping, and our measurements provide a direct evidence of its validity. Our analysis is generalized to any arbitrary delayed force, and it is not limited to the bolometric pressure alone. It can be shown that for any given type of photon-induced force $F_n(z)$, the condition for optimal damping is obtained when both the photon-induced rigidity equals the lever rigidity (that is, $K_n = -K$) and the time constant of the force is of the order of the lever period (that is, $\tau_n = \sqrt{2}/\omega_0$). Ideally then, effective temperature can be lowered to a minimum of $T_{\text{eff}}/T = 4\sqrt{2}/Q_M$. The best cooling is therefore obtained for large Q_M . In vacuum and at low temperatures, Q_M can be made as large as 10^5 , which means that sub-millikelvin effective temperatures are in principle possible when starting from a surrounding temperature in the sub-kelvin range.

In our particular example, for which cooling is controlled through bolometric effects, the brownian motion data measured in the laser-cooling regime in Fig. 2, and analysed with equation (5) and (7), correspond to a reduced temperature as low as $T_{\text{eff}} \approx 18 \text{ K}$

down from room temperature. In principle, the limit of cavity cooling is reached when the heating resulting from the light power absorbed in the lever mirror exceeds the cooling power. In our experiment, this situation was still not reached for an effective cooling of 18 K. Increasing the cavity reflectivity increases the contribution of radiation pressure to the optical damping. This is because in a low-loss FP cavity with a mirror separation L and with high reflectivity R (that is, high finesse), the radiation pressure does not change instantaneously with the lever motion—instead it is delayed by the cavity storage time $\tau_R = L/[c(1-R)]$. In such an ideal cavity, the lever cooling is analogous to that of atomic molasses. The analogy is revealed when we compare the expression of the velocity-dependent forces determined for (1) an atom placed in counter-propagating laser beams and (2) for the lever subject to the retarded radiation pressure in the cavity. In both cases, we determine that the optically induced damping rate at frequency ω is given by

$$\Gamma_{\text{opt}} = \frac{S_0 \sigma}{mc^2} \frac{\Omega \tau}{\omega^2 \tau^2 + 1} \left\{ \frac{4\delta\tau}{(1 + 4\tau^2 \delta^2)^2} \right\} \quad (8)$$

where S_0 is the laser total power density, $\Omega = 2\pi\nu$, where ν is the photon frequency with wavelength λ , and m is the atom or lever mass. The delay time τ corresponds to the radiative lifetime of the atom optical transition, whereas for the lever it is the cavity storage time τ_R . Here σ has the dimension of area. For atoms, it is the optical scattering cross-section at the optical transition frequency, namely $\sigma = 3\lambda^2/2\pi$. For the FP cavity, the cross-section is instead $\sigma \approx 8RA/(1-R)^2$, where A is the illuminated area on the lever.

The term in parentheses in equation (8) is simply a numerical function of δ , the frequency detuning from optical resonance. It takes the value 0 for $\delta = 0$ on cavity resonance, and has the maximum value $+3\sqrt{3}/8$ for a red-shift detuning $\delta_- = -1/(2\sqrt{3}\tau)$. At this detuning under a laser power P_0 , we derived that the lever vibrational effective temperature is:

$$T_{\text{eff}} = \frac{T}{\left[1 + 6\pi\sqrt{3} \frac{P_0/\Gamma}{mc^2} \frac{L R(1+R)}{\lambda(1-R)^3} \frac{1}{1+\omega_0^2 \tau_R^2} \right] \left[1 - \frac{3\sqrt{3} P_0/\omega_0}{2} \frac{\Omega}{mc^2} \frac{R\sqrt{R}}{\omega_0(1-R)^2} \frac{1}{1+\omega_0^2 \tau_R^2} \right]} \quad (9)$$

In the denominator, the first term in brackets originates from the cavity-induced damping, while the second term is due to the cavity-induced rigidity. For $T_{\text{eff}} \ll T$, the optimal working point is given at frequency $\omega_0\tau_R \approx 1$, namely $\omega_0 \approx c(1-R)/L$, and the lever thermal energy in units of the vibrational quantum is then minimized down to:

$$\frac{k_B T_{\text{eff}}}{\hbar\omega_0} \cong \frac{2}{3\sqrt{3}} \frac{k_B T}{\hbar\Omega} \frac{mc^2}{P_0/\Gamma} \frac{(1-R)^2}{R} \quad (10)$$

The quantum limit is reached for $k_B T_{\text{eff}} < \hbar\omega_0$. Using a mechanical resonator (with a mass $m = 2.5 \times 10^{-15} \text{ kg}$ and a natural damping rate of $\Gamma \approx 20 \text{ Hz}$) made of a tiny $1 \times 1 \times 1 \mu\text{m}^3$ sized Bragg dielectric mirror with $R = 0.99$ placed in a cavity with $L = 20 \text{ cm}$ and illuminated with $P_0 = 2 \mu\text{W}$ and $\lambda = 1 \mu\text{m}$ would lead to a temperature reduction of 1/5,000 at 400 kHz. For a lever pre-cooled to $T = 100 \text{ mK}$, the added optical cooling would leave it in its quantum limit should its vibrational frequency be between 400 kHz and 10 MHz. Here, as in the case of bolometric cooling, the potential limitation is reached when the residual optical absorption in the lever heats it more than it cools it. Whether the quantum limit or the residual optical thermal heating of the vibrational mode is reached first remains to be experimentally investigated. \square

Received 27 June; accepted 18 October 2004; doi:10.1038/nature03118.

1. Marshall, W., Simon, C., Penrose, R. & Bouwmeester, D. Toward quantum superpositions of a mirror. *Phys. Rev. Lett.* **91**, 130401 (2003).
2. Cohadon, P. F., Heidmann, A. & Pinard, M. Cooling of a mirror by radiation pressure. *Phys. Rev. Lett.* **83**, 3174–3177 (1999).
3. Wilson-Rae, I., Zoller, P. & Imamoglu, A. Laser cooling of a nanomechanical resonator mode to its

quantum ground state. *Phys. Rev. Lett.* **92**, 075507 (2004).

4. Mertz, J., Marti, O. & Mlynek, J. Regulation of a microlever responses by force feedback. *Appl. Phys. Lett.* **62**, 2344–2346 (1993).
5. Hänsch, T. W. & Schawlow, A. Cooling of gases by laser radiation. *Opt. Commun.* **13**, 68–69 (1975).
6. Cohen-Tannoudji, C. & Phillips, W. New mechanisms for laser cooling. *Phys. Today* **43**, 33–52 (1990).
7. Chu, S., Hollberg, L., Björholm, J. E., Cable, A. & Ashkin, A. Three-dimensional viscous confinement and cooling of atoms by resonance radiation pressure. *Phys. Rev. Lett.* **55**, 48–51 (1985).
8. Epstein, R. L., Buchwald, M. L., Edwards, B. C., Gosnell, T. R. & Mungan, C. E. Observation of laser-induced fluorescent cooling of a solid. *Nature* **377**, 500–502 (1995).
9. Braginsky, V. B. & Manukin, A. B. *Measurements of Weak Forces in Physics Experiments* (Chicago Univ. Press, Chicago, 1977).
10. Braginsky, V. B., Manukin, A. B. & Tikhonov, M. Yu. Investigation of dissipative ponderomotive effects of electromagnetic radiation. *Zh. Eksp. Teor. Fiz.* **58**, 1549–1552 (1970); *Sov. Phys. JETP* **31**, 829–830 (1970).
11. Dorsel, A., McCullen, J. D., Meystre, P., Vignes, E. & Walther, H. Optical bistability and mirror confinement induced by radiation pressure. *Phys. Rev. Lett.* **51**, 1550–1553 (1983).
12. Vogel, M., Mooser, C., Karrai, K. & Warburton, R. Optically tunable mechanics of microlevers. *Appl. Phys. Lett.* **83**, 1337–1339 (2003).
13. Sarid, D. *Scanning Force Microscopy* (Oxford Univ. Press, New York, 1991).
14. Gillespie, D. T. The mathematics of Brownian motion and Johnson noise. *Am. J. Phys.* **64**, 225–240 (1996).
15. Gimzewski, J. K., Gerber, Ch., Meyer, E. & Schlitter, R. R. Observation of a chemical reaction using a micromechanical sensor. *Chem. Phys. Lett.* **217**, 589–594 (1994).
16. Barnes, J. R., Stephenson, R. J., Welland, M. E., Gerber, Ch. & Gimzewski, J. K. Photothermal spectroscopy with femtojoule sensitivity using a micromechanical device. *Nature* **372**, 79–81 (1994).
17. Datskos, P. G., Lavrik, N. V. & Rajic, S. Performance of uncooled microcantilever thermal detectors. *Rev. Sci. Instrum.* **75**, 1134–1148 (2004).
18. Yang, J., Ono, T. & Esashi, M. Surface effects and high quality factor in ultrathin single-crystal silicon cantilever. *Appl. Phys. Lett.* **77**, 3860–3862 (2000).
19. Pai, A., Dhurandhar, S. V., Hello, P. & Vinet, J. Y. Radiation pressure induced instabilities in laser interferometric detectors of gravitational waves. *Eur. Phys. J. D* **8**, 333–346 (2000).

Acknowledgements We thank T. Hänsch, A. Imamoglu, R. Warburton and S. Huant for discussions. The Deutsche Forschungsgemeinschaft (DFG) funded this work.

Competing interests statement The authors declare that they have no competing financial interests.

Correspondence and requests for materials should be addressed to K.K. (karrai@imu.de).

Plasma devices to guide and collimate a high density of MeV electrons

R. Kodama¹, Y. Sentoku², Z. L. Chen¹, G. R. Kumar^{1*}, S. P. Hatchett³, Y. Toyama¹, T. E. Cowan², R. R. Freeman¹, J. Fuchs^{2*}, Y. Izawa¹, M. H. Key³, Y. Kitagawa¹, K. Kondo⁵, T. Matsuoka¹, H. Nakamura¹, M. Nakatsutsumi¹, P. A. Norreys⁶, T. Norimatsu¹, R. A. Snavely³, R. B. Stephens⁷, M. Tampo¹, K. A. Tanaka⁵ & T. Yabuuchi¹

¹Institute of Laser Engineering, Osaka University, 2-6 Yamada-oka, Suita Osaka 565-0871, Japan

²University of Nevada, Department of Physics, MS-220, Reno, Nevada 89557, USA

³University of California, Lawrence Livermore National Laboratory, PO Box 808, Livermore, California 94550, USA

⁴The Ohio State University, Columbus, Ohio 43210, and University of California, Davis, Department of Applied Science, Livermore, California 94550, USA

⁵Faculty of Engineering and Institute of Laser Engineering Osaka University, 2-6 Yamada-oka, Suita Osaka 565-0871, Japan

⁶Rutherford Appleton Laboratory, Chilton, Didcot, Oxon, OX11 0QX, UK

⁷General Atomics, San Diego, California 92186, USA

* Permanent addresses: Tata Institute of Fundamental Research, Mumbai 400 005, India (G.R.K.); Laboratoire pour l'Utilisation des Lasers Intenses, UMR 7605 CNRS-CEA-École Polytechnique-Univ. Paris VI, 91128 Palaiseau, France (J.F.)

The development of ultra-intense lasers¹ has facilitated new studies in laboratory astrophysics² and high-density nuclear science³, including laser fusion^{4–7}. Such research relies on the efficient generation of enormous numbers of high-energy charged particles. For example, laser–matter interactions

at petawatt (10^{15} W) power levels can create pulses of MeV electrons^{8–10} with current densities as large as 10^{12} A cm⁻². However, the divergence of these particle beams⁵ usually reduces the current density to a few times 10^6 A cm⁻² at distances of the order of centimetres from the source. The invention of devices that can direct such intense, pulsed energetic beams will revolutionize their applications. Here we report high-conductivity devices consisting of transient plasmas that increase the energy density of MeV electrons generated in laser–matter interactions by more than one order of magnitude. A plasma fibre created on a hollow-cone target guides and collimates electrons in a manner akin to the control of light by an optical fibre and collimator. Such plasma devices hold promise for applications using high energy-density particles and should trigger growth in charged particle optics.

Electron beams with enormous energy density can be guided by a high-conductivity device consisting of transient high-density plasmas, as the forward-directed energetic electron current can be compensated by a high-density return current in these plasmas. Shaped-plasma devices, such as the hollow-cone and fine fibre-like plasmas shown in Fig. 1a, guide and collimate the high-density energetic-electron beam generated by ultra-intense laser light. Figure 1a shows the electric field contours in the shaped plasma at different times, as generated by a two-dimensional particle-in-cell (PIC) simulation¹¹, showing the electron propagation being accompanied by the fields. Ultra-intense laser light (8×10^{18} W cm⁻²) is injected into the hollow cone, and generates high-density MeV electrons with an average energy of 3.3 MeV at the tip of the cone. These electrons propagate along the hollow cone's interior surface¹¹ and in the fibre-like plasma. The large current is compensated by the return current set up by the high-density electrons inside the bulk of the fibre.

Propagation (with an angular spread) of the high-density MeV electrons outside the fibre-like plasma induces a strong radial electric field (E_y ; TV m⁻¹) surrounding the fibre-like plasmas (Fig. 1b), and acts to pinch the MeV electrons along the fibre length. A strong azimuthal magnetic field (B_z) of the order of a few hundred MG is also created, and this diverts the MeV electron propagation. The maximum E_y and B_z are given by $E_y = 4\pi eN_e$ and $B_z = 4\pi eN_e(v_e/c)$, respectively. Here N_e is number of electrons surrounding the wire, and v_e is the hot electrons' mean velocity. When the electron velocity is close to the speed of light c , the electric force eE_y and the magnetic force $e(v_e/c)B_z \approx eB_z$ are balanced. Therefore the fast electrons, which are pushed outside by the magnetic field, are returned into the wire by the sheath fields. This field balance results in the collimation and confinement of the electrons in the fibre-like plasmas. Such MeV electron guiding and collimation in the hollow-cone¹¹ and fibre-like plasmas are clearly seen in the electron trace images shown in Fig. 1c. The electrons propagate along the wire with an oscillation due to the surrounding electric and magnetic fields. During the propagation, the transverse emittance of the beam is also reduced by a loss of its transverse energy to the bulk plasma and/or energetic ions via the radial electric field, resulting in beam cooling, which may be analogous to mode selection of light with a single-mode fibre.

We now experimentally demonstrate guiding and collimation of the high-density MeV electrons in the fibre-like plasma device by using a fine carbon wire (5 μm diameter and 1 mm length) attached to a hollow-cone target⁵ (Fig. 2a). The size of the target in the experiment is not comparable to the condition in the simulation code. However, the guiding and collimation of the electrons predicted by the simulation is qualitatively proved by using the target shown in Fig. 2a in the experiments. Laser light (250–300 TW, 0.6–0.8 ps) with an energy of 180 J (ref. 12) was injected into the cone and focused at the tip of the cone. The hollow-cone side wall can guide the laser light and electrons to the 30-μm tip of the cone, resulting in the enhancement of the MeV electron flux by a factor of